

Effects of Hydrolysis on Force Generation by Actin Filaments

A. E. Carlsson

Department of Physics, Washington University, St. Louis, MO 63130

(Dated: October 1, 2007)

Abstract

The effects of ATP hydrolysis on actin polymerization-based force generation are calculated using a multistate two-state Brownian-ratchet model based on measured polymerization curves. For ensembles of filaments pushing against a rigid obstacle, the stall force per filament can be much less than the equilibrium ATP-actin stall force.

PACS numbers: 87.15.Rn,87.17.Jj,87.16.Ac,87.15.Cc

Cell motility and shape changes rely crucially on force generation by polymerization of the protein actin into semiflexible filaments [1, 2]. These filaments have growing “barbed” ends and depolymerizing “pointed” ends. In the widely accepted “Brownian-ratchet” (BR) theory [3], opposing force slows monomer addition by reducing the space available for free monomers to diffuse to the barbed end. The stall force of a filament is determined the competition between depolymerization and polymerization. In equilibrium, it is

$$F_{\text{eq}} = \frac{k_{\text{B}}T}{a} \ln(G/G_{\text{c}}^{\text{B}}), \quad (1)$$

where a is the length increment per added subunit, G is the free-monomer concentration, and G_{c}^{B} is the barbed-end critical concentration - the free-monomer concentration at which barbed-end polymerization and depolymerization balance each other [4]. Efficient disassembly of polymerized actin is also essential for continued cell motion. This results either directly or indirectly from hydrolysis, during which a molecule of adenosine triphosphate (ATP) bound to an actin subunit in a filament is converted to adenosine diphosphate (ADP). Hydrolysis enhances depolymerization. For ATP-actin, $G_{\text{c}}^{\text{B}} \simeq 0.1\mu\text{M}$, while for ADP-actin, $G_{\text{c}} \simeq 2\mu\text{M}$ [5]. The effect of hydrolysis on the measured polymerization velocity [6] V (the net rate of subunit addition) is seen in Figure 1. At high concentrations, V grows linearly with G as expected from standard polymerization theory [7]. At lower concentrations, V turns sharply negative, indicating a transition to a rapidly depolymerizing state. Several theoretical models [8–10] have attributed this behavior to an “ATP cap” [11]: a finite number of barbed-end subunits which have not had time to hydrolyze. The ATP cap grows with increasing G above G_{c}^{B} . When G drops below G_{c}^{B} , the cap shrinks, and the probability for the tip to be ADP-bound grows, causing rapid depolymerization.

Since opposing force reduces the monomer on-rate, it will also reduce the ATP cap, shifting the tip state toward depolymerization. This effect will enhance the sensitivity of V to opposing force, and thus reduce the stall force. I explore this effect using a multifilament two-state BR growth model, having growing and shrinking states. A filament is described by L , the number of subunits it contains, and I_{tip} , which is 1 for the depolymerizing ADP-tip state, and 2 for the polymerizing ATP-tip state. This model does not treat the detailed molecular nature of the tip states, such as the number of subunits in the ATP cap. Nor does it distinguish between the ADP and intermediate ADP- P_i states. However, it does describe correctly the dependence of V on G . Because force reduces the monomer addition rate, the

G-dependence of V is closely related to its force dependence. I assume that the monomeric actin is all ATP-bound. The following transitions and rates are treated:

$$\begin{aligned}
(L, 2) &\rightarrow (L + 1, 2) : k_{\text{on}}^{22} \\
(L, 2) &\rightarrow (L - 1, 2) : k_{\text{off}}^{22} \\
(L, 1) &\rightarrow (L - 1, 1) : k_{\text{off}}^{11} \\
(L, 1) &\rightarrow (L + 1, 2) : k_{\text{on}}^{21} \\
(L, 2) &\rightarrow (L - 1, 1) : k_{\text{off}}^{12}
\end{aligned} \tag{2}$$

Here k_{on}^{22} describes polymerization in state 2, and I take $k_{\text{on}}^{22} = k_{\text{on},0}^{22}G$, where $k_{\text{on},0}^{22} = 11.6\mu\text{M}^{-1}\text{s}^{-1}$ [5]. The corresponding off-rate k_{off}^{22} is assigned a G-independent value $k_{\text{off}}^{22} = G_c^B k_{\text{on},0}^{22} = 1.16\text{s}^{-1}$, using the typical value $G_c^B = 0.1\mu\text{m}$. I ignore $1 \rightarrow 1$ transitions involving monomer addition, since these would require instantaneous hydrolysis. I take $k_{\text{off}}^{11} = 5.4\text{s}^{-1}$ [5]. As in previous work [9, 10], I assume that $1 \rightarrow 2$ changes of the tip state occur only by addition of a new ATP subunit, at a rate $k_{\text{on}}^{21} = k_{\text{on},0}^{21}G$. The value of $k_{\text{on},0}^{21}$ is not known, but the results are insensitive to its value, with a factor of ten change in $k_{\text{on},0}^{21}$ changing the stall force by less than 20%. Thus, for simplicity, I take $k_{\text{on},0}^{21} = k_{\text{on},0}^{22}$.

I also assume that $2 \rightarrow 1$ transitions occur only by depolymerization (k_{off}^{12}). I have also performed calculations in which such changes occur without depolymerization, and the forces change by less than 20%. Because the precise nature of states 1 and 2 is not known, one cannot deduce k_{off}^{12} directly from measured rate parameters. However, the relative probabilities of the tip being in the two states can be determined from the V vs. G data of Fig. 1. In the two-state model, $V = (1 - P_2)V_1 + P_2V_2$, where $V_{1,2}$ are the velocities in states 1 and 2, and P_2 is the probability of being in state 2. Therefore, $P_2 = [V - V_1]/[V_2 - V_1]$. I regard V_1 as constant and V_2 as having a linear dependence on G . Then, using the fit to the measured $V(G)$ points for $G < G_c^B$ to calculate $P_2(G)$, I find that the form

$$P_2(G) = G/G_c^B. \tag{3}$$

is accurate. On the other hand, P_2 constrains the model parameters as follows:

$$P_2(G) = \frac{k_{\text{on}}^{21}}{k_{\text{on}}^{21} + k_{\text{off}}^{12}}. \tag{4}$$

I thus use a concentration-dependent conversion rate

$$k_{\text{off}}^{12}(G) = k_{\text{on}}^{21}(G)[1/P_2(G) - 1] = k_{\text{on},0}^{21}(G_c^B - G) \tag{5}$$

for $G < G_c^B$; $k_{\text{off}}^{12}(G)$ vanishes for $G > G_c^B$. This gives a good fit to the data in Fig. 1.

The model for obstacle propulsion is shown in Fig. 2. I treat N rigid filaments, aligned parallel to each other, pushing in the x -direction on a rigid obstacle whose position x_{obst} is described by a probability distribution $\rho(x_{\text{obst}})$. The tip of the m -th filament is at $x_m = aL_m + \delta_m$, where $a = 2.7nm$ is the length added per subunit, and the fractional shift between filaments $\delta_m = (m-1)a/N$ is included to account for the filaments being out of step at their bases. For definiteness, I assume that the obstacle is held in a laser trap of spring constant k_{spr} , centered at $x_{\text{obst}} = 0$, so that the external force acting on it is $F = k_{\text{spr}}x_{\text{obst}}$, where positive F is taken to be in the $-x$ direction. The obstacle is taken to have an infinite diffusion constant and x_{obst} must be greater than x_{max} , the maximum of the x_m . These assumptions imply that to a very good approximation

$$\rho(x_{\text{obst}}) \propto \exp [-(x_{\text{obst}} - x_{\text{max}})F/k_{\text{B}}T], \quad (6)$$

over the range of obstacle positions defined by $k_{\text{spr}}(x_{\text{obst}} - x_{\text{max}})^2 \ll k_{\text{B}}T$, which includes most of the range relevant for our simulations.

The effect of the obstacle on the rates is treated via the effective force-dependent free-actin concentration

$$G_{\text{eff}} = p_{\text{open}}G, \quad (7)$$

where p_{open} (which depends on m) is the probability that $x_{\text{obst}} - x_m > a$. Eq. (6) implies that

$$p_{\text{open}} = \exp [(-a + x_{\text{max}} - x_m)F/k_{\text{B}}T] \quad (8)$$

if $x_{\text{max}} - x_m < a$, and $p_{\text{open}} = 1$ otherwise. In the obstacle simulations I replace G by G_{eff} everywhere, to account for the slowing of polymerization by opposing force. Since k_{off}^{12} is nonzero only when $G_{\text{eff}} < G_c^B$, Eqs. (8) and (7) imply that the “1” state “turns on” only when F exceeds F_{eq} , as calculated for for the polymerizing “2” state.

The multifilament growth process is treated via the Gillespie method [12], in which The timestep is determined stochastically. After each event, x_{max} is reevaluated, and $\rho(x_{\text{obst}})$ is shifted if necessary. The filaments start at zero length, and grow until x_{max} reaches a constant plateau \bar{x}_{max} . The force per filament is then $k_{\text{spr}}\bar{x}_{\text{max}}/N$. Most of the simulations use a concentration $G=1.67G_c^B$ and a spring constant $k_{\text{spr}} = 0.008pN/nM$, motivated by recent measurements [13] of force generation. Part of a typical trajectory for a single filament

of an $N=10$ ensemble is shown in Fig. 3a (thinner line) along with the obstacle trajectory (thicker line). The filament trajectory displays a cycle in which the filament contacts the obstacle, changes state and depolymerizes, is rescued into the polymerizing state, and once again contacts the obstacle. Fig. 3b shows the stall force per filament for small ensembles. For $N = 1$, a reduction of 10-15% relative to F_{eq} occurs, because fluctuations in the filament tip position occasionally move the obstacle into regions where $F > F_{\text{eq}}$, causing transitions into the “1” state. If k_{spr} is much smaller, F is essentially constant, and the single-filament force is much closer to F_{eq} . I note that the presence of hydrolysis invalidates equilibrium analysis, so that deviations from F_{eq} are to be expected.

For larger N , the force per filament drops by about a factor of three. This occurs because the force fluctuations experienced by a given filament are larger. Most of the time, a given filament carries no force at all because the obstacle force is being carried by other filaments; during the remaining time the filament is carrying the whole obstacle load or a large fraction of it. Such a large force can rapidly cause $2 \rightarrow 1$ transitions because it reduces G_{eff} and thereby increases k_{off}^{12} (see Eq. (5)). This effect is much less sensitive to k_{spr} than the smaller effect seen for single filaments, with factor-of-five changes in k_{spr} causing less than 2% changes in the stall force. As the number of filaments becomes very large (data not shown), the force per filament approaches an asymptotic value about four times less than F_{eq} .

The behavior seen here is closely analogous to that hypothesized by Footer *et al* [13] on the basis of their optical-trap experiments, in which 6-8 filaments exerted forces on a fixed obstacle. The filaments grew from the tip of an acrosome-bead complex held in an optical trap with $k_{\text{spr}} = 0.008pN/nm$. This experimental geometry is equivalent to the one considered here, since in both cases the relative position of the obstacle and the filaments fluctuates in the force field generated by the optical trap. Standard hydrodynamic results [14] for spheres and thin rods show that the drag coefficients of the $2\mu m$ bead and the $8\mu m$ bundle are comparable, with that of the sphere being larger. Taking the drag coefficient of the complex to be twice the drag coefficient of a $2\mu m$ bead, assuming a viscosity equal to that of water, and using the Einstein relation [14] to obtain the diffusion coefficient, gives a diffusion coefficient of $10^5 nm^2/s$ for the complex. Then the time required for the complex to diffuse the distance a is $(2.7nm)^2/(2 \times 10^5 nm^2/s) = 4 \times 10^{-5}s$. On the other hand, the actin concentrations of $1 - 4\mu m$ and on-rate constant of $2.9\mu M^{-1}s^{-1}$ in Ref. 13 imply

monomer addition times of 0.1 s to 0.3 s, which greatly exceed the diffusion time. Therefore the obstacle diffusion can be regarded as infinitely rapid, as in the simulations.

The experiments were performed in a medium of profilin-actin to maintain a sufficient supply of free actin monomers. Several actin concentrations were used, but only at the lowest (1.67 times the apparent barbed-end critical concentration in the presence of profilin) could filament buckling be safely ignored. At this concentration, the total forces measured from the displacement of the acrosome were closer to F_{eq} than to NF_{eq} . On this basis, it was suggested that only one or two filaments at a time contact the obstacle, and that the filaments “trade off”, going through cycles of polymerization and depolymerization. This is precisely the scenario seen in the present simulations.

I am not able to simulate this system quantitatively because the kinetic parameters for the conditions of the experiment are not sufficiently well known. But in order to establish which parameters are most important for the force reduction, I present an analytic theory of the force exerted by a single fixed filament growing against an immovable obstacle, with $G > G_c^B$. This case is similar to the several-filament case in that the filament will go through periods of contact interrupted by excursions away from the obstacle. My simulations of this system give force reductions similar to those in the many-filament simulations for large N . The theory treats the filament “growth cycle” illustrated in Fig. 4. The filament starts in state 2 in contact with the obstacle. Once it switches to state 1, it leaves the obstacle and remains in state 1 for a time T_{21} . The distance to the obstacle (measured in subunits) is then $T_{21}k_{\text{off}}^{11}$. After it switches back to state 2, the time to return to the obstacle is $T_{21}k_{\text{off}}^{11}/(k_{\text{on}}^{22} - k_{\text{off}}^{22})$. When it reaches the obstacle it remains in contact with it (i. e. within a few subunits of the obstacle) for a time T_{12} until it switches to state 1. During this time I assume that it generates a force F_{eq} . The average force generated by the filament is thus

$$\bar{F} = F_{\text{eq}} \frac{T_{12}}{T_{12} + T_{21}[1 + k_{\text{off}}^{11}/(k_{\text{on}}^{22} - k_{\text{off}}^{22})]}. \quad (9)$$

To evaluate \bar{F} , I take $T_{21} = 1/k_{\text{on},0}^{21}G$, where G is used rather than G_{eff} since the $1 \rightarrow 2$ transition occurs far from the obstacle. To obtain T_{12} , I note that during the time the filament is in state 2 in the vicinity of the obstacle, it undergoes alternating polymerization and depolymerization steps. Immediately after a depolymerization step, x_m is far enough from x_{obst} that $G_{\text{eff}} = G$, so filament growth is favored and I ignore back-to-back depolymerization steps; then back-to-back polymerization steps are also absent because of the hard obstacle.

Immediately after a polymerization step, there is no more room to add another subunit, so $G_{\text{eff}} = 0$; then Eq. (5) shows that $k_{\text{off}}^{12} = k_{\text{on},0}^{21} G_c^B$. The probability p_b that the filament tip is in this blocked state is determined by the balance between (net) polymerization leading to unblocking, and depolymerization leading to blocking: $p_b = (k_{\text{on}}^{22} - k_{\text{off}}^{22}) / [k_{\text{off}}^{22} + (k_{\text{on}}^{22} - k_{\text{off}}^{22})] = 1 - G_c^B / G$. Therefore, $T_{21} / T_{12} = p_b k_{\text{on},0}^{21} G_c^B / k_{\text{on},0}^{21} G = (G_c^B / G)(1 - G_c^B / G)$, and

$$\begin{aligned} \bar{F} &= \frac{F_{\text{eq}}}{1 + [(G_c^B / G)(1 - G_c^B / G)][1 + k_{\text{off}}^{11} / (k_{\text{on}}^{22} - k_{\text{off}}^{22})]} \\ &= \frac{F_{\text{eq}}}{1 + (G_c^B / G)[(1 - G_c^B / G) + k_{\text{off}}^{11} / k_{\text{on}}^{22}]} \end{aligned} \quad (10)$$

In the simulations, $G / G_c^B = 1.67$ and $k_{\text{off}}^{11} / k_{\text{on}}^{22} = 2.8$, so that $\bar{F} = 0.34 F_{\text{eq}}$, a reduction similar to that in seen in Fig. 3.

Eq. (10) shows that large values $k_{\text{off}}^{11} / k_{\text{on}}^{22}$ will lead to force reduction. While k_{on}^{22} was determined in Ref. 13, I am not aware of measurements of k_{off}^{11} for similar conditions. The theory proposed here could be tested by correlating the force per filament with the number of filaments in optical-trap experiments. If the present theory is valid, the force per filament will be smaller for larger numbers of filaments, as indicated in Fig. 3.

The calculations presented here show that when ATP hydrolysis is present, an ensemble of actin filaments growing against a rigid obstacle can have a stall force much less than $N F_{\text{eq}}$. This finding is based on the measured polymerization properties of actin filaments, and does not assume specific molecular-level processes determining the ATP cap. The force reduction occurs under conditions where actin filaments can switch between growing and rapidly depolymerizing states. It is most pronounced at low actin concentrations. In biological cells, the assumptions of the model, namely a rigid obstacle and parallel filaments, render it most applicable to the tips of growing filopodia, thin protrusions driven by parallel actin bundles. Here the close spacing of filaments reduces the effects of the membrane flexibility. At the filopodial tips, G is reduced by depletion of free monomers [15]. Therefore force available for extending filopodia could be much less than F_{eq} .

I am grateful to Frank Brooks for a careful reading of this paper, and to the Aspen Center for Physics for a two-week stay during which this work was initiated. This work was supported by the National Science Foundation under Grant DMS-0240770.

[1] D. Bray, *Cell Movements: from Molecules to Motility* (Garland Publishing, New York, 2001).

- [2] T. D. Pollard and G. G. Borisy, *Cell* **112**, 453 (2003).
- [3] C. S. Peskin, G. M. Odell, and G. F. Oster, *Biophys. J.* **65**, 316 (1993).
- [4] T. L. Hill and M. W. Kirschner, *Int. Rev. Cytol.* **78**, 1 (1982).
- [5] K. Fujiwara, D. Vavylonis, and T. D. Pollard, *Proc. Nat. Acad. Sciences USA* **104**, 8827 (2007).
- [6] M. F. Carrier, D. Pantaloni, and E. D. Korn, *J. Biol. Chem.* **261**, 10785 (1986).
- [7] F. Oosawa, *Thermodynamics of the Polymerization of Protein* (Academic Press, New York, 1975).
- [8] T. L. Hill, *Biophys. J.* **49**, 981 (1986).
- [9] D. Vavylonis, Q. Yang, and B. O'Shaughnessy, *Proc. Nat. Acad. Sciences USA* **102**, 8543 (2005).
- [10] E. B. Stukalin and A. B. Kolomeisky, *Biophys. J.* **90**, 2673 (2006).
- [11] M.-F. Carrier, D. Pantaloni, and E. D. Korn, *J. Biol. Chem.* **259**, 9983 (1984).
- [12] D. T. Gillespie, *J. Comput. Phys.* **22**, 403 (1976).
- [13] M. J. Footer, J. W. J. Kerssemakers, J. A. Theriot, and M. Dogterom, *Proc. Nat. Acad. Sciences USA* **104**, 2181 (2007).
- [14] M. Doi and S. F. Edwards, *The Theory of Polymer Dynamics* (Clarendon Press, Oxford, 1998).
- [15] A. Mogilner and B. Rubinstein, *Biophys. J.* **89**, 782 (2005).

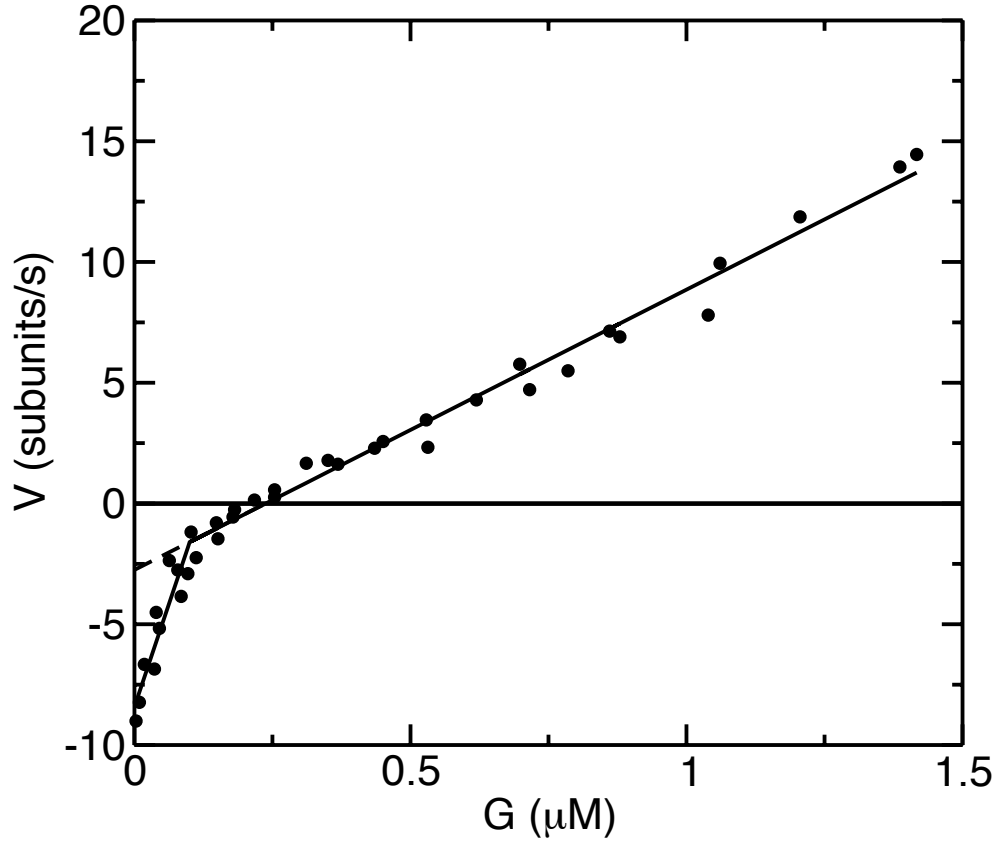


FIG. 1: Piecewise linear fit to growth velocity vs. free-actin concentration G digitized from Fig. 1 of Ref. 6. Vertical scale is obtained by assuming an on-rate constant of $11.6\mu M^{-1}s^{-1}$ (Ref. 5). Lines are separate least-squares fits to the data above and below G_c^B . Dashed line is extrapolation of $G > G_c^B$ results to $G < G_c^B$.

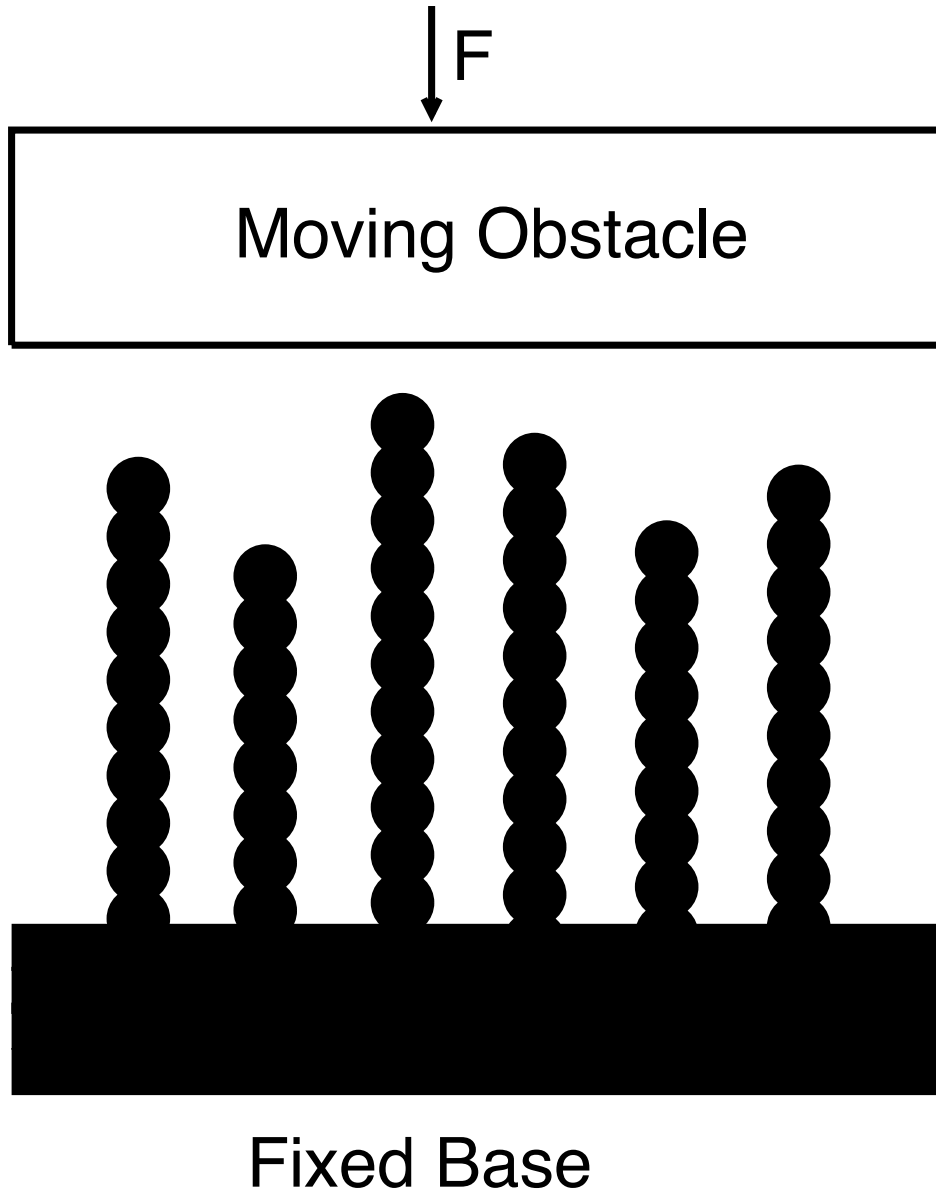


FIG. 2: Schematic of many-filament growth model.

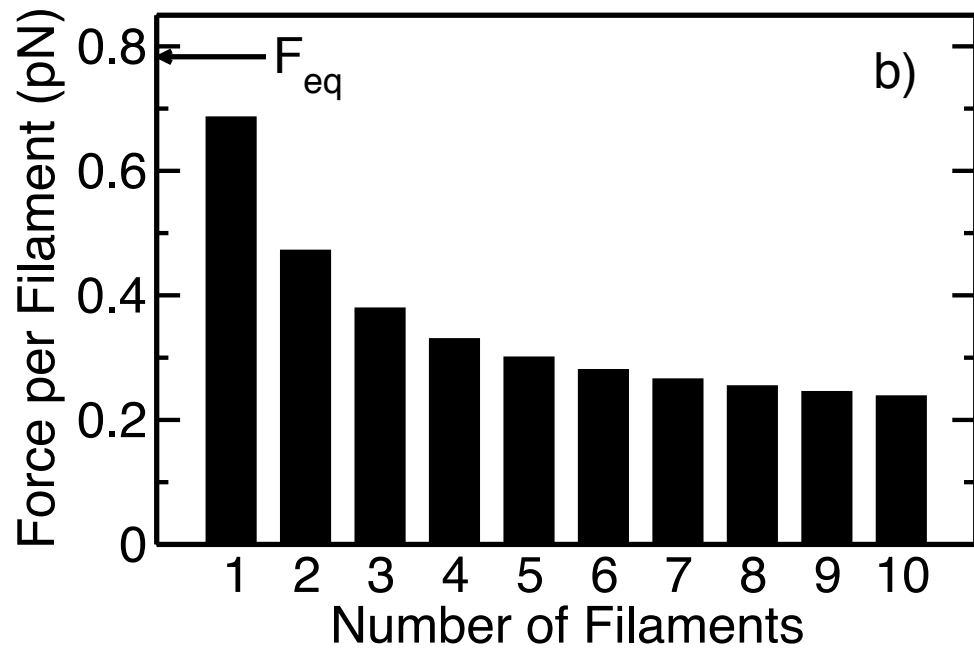
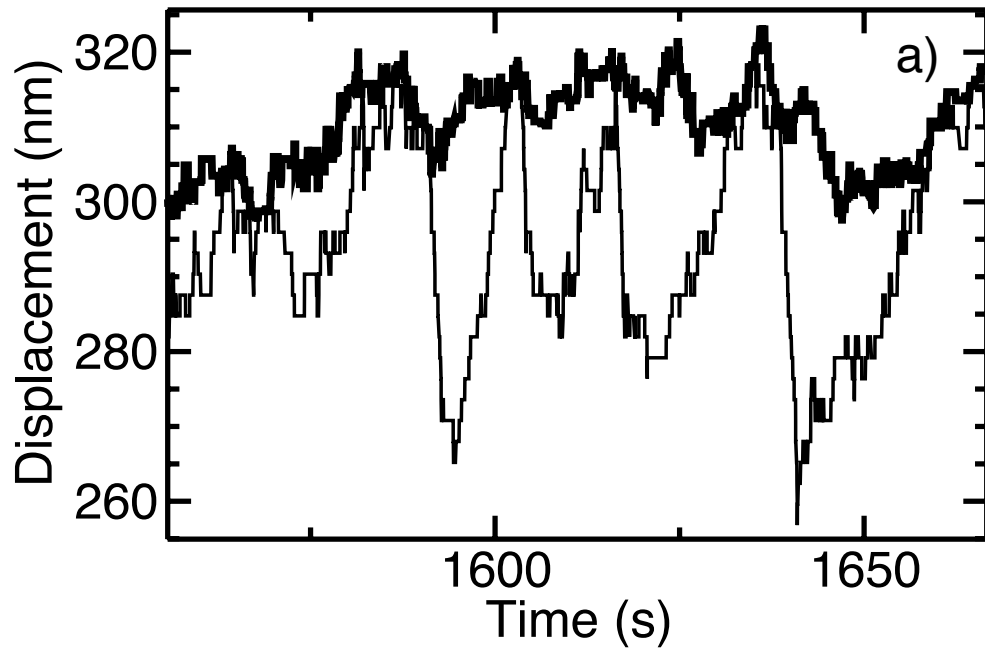


FIG. 3: a) Part of trajectory of obstacle baseline position (thick line) and position of a single filament tip (thin line) in simulation for ten filaments. b) Force per filament as function of number of filaments pushing obstacle.

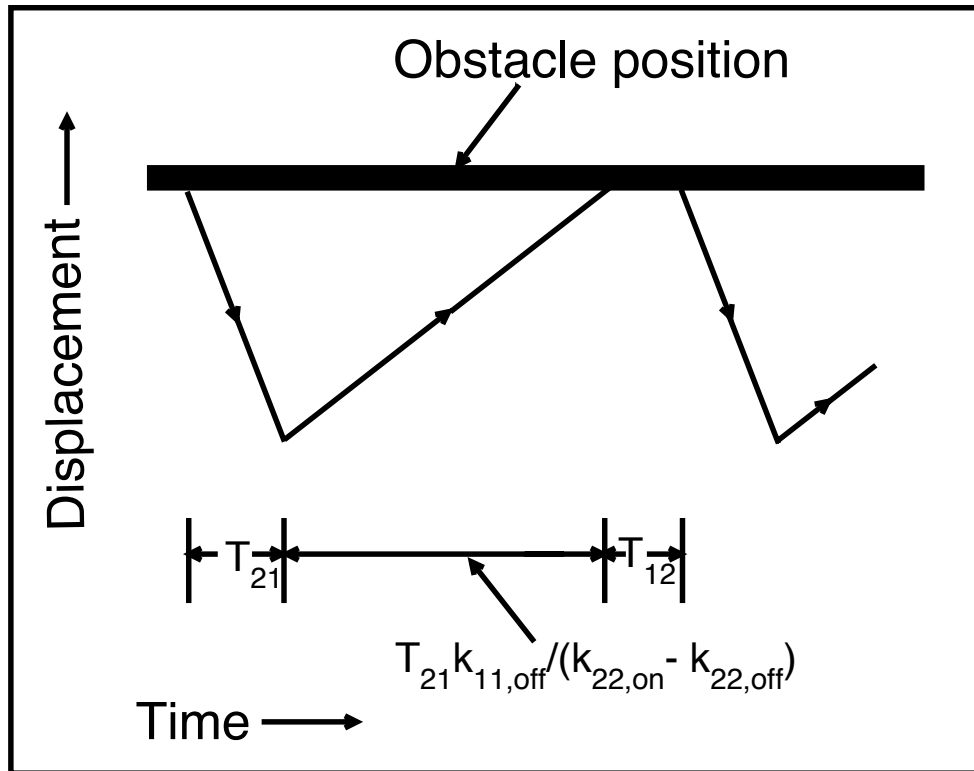


FIG. 4: Schematic of model for filament growth against fixed obstacle.